RESEARCH ARTICLE OPEN ACCESS

Growth and Characterization of ADP Single Crystals Added With CdS

J. Anitha Hudson[1], C.K. Mahadevan[2] and C.M. Padma[3]
[1,3] (Department of Physics, Women's Christian College, Nagercoil - 629 001,Tamil Nadu, India)
[2] (Physics Research Centre, S.T. Hindu College, Nagercoil - 629 002, Tamil Nadu, India)

ABSTRACT
Pure and CdS added (in five concentrations) ammonium dihydrogen orthophosphate (ADP) single crystals have been grown at room temperature by the free evaporation method. The six grown crystals have been characterized structurally, chemically, thermally, mechanically, optically and electrically using the available standard methods. The powder X-ray diffraction and Fourier transform infrared spectral measurements confirm the crystal and molecular structures. The atomic absorption spectroscopic measurement confirms the presence of impurity in the CdS added crystals. Thermogravimetric, UU-Vis-NIR spectral and microhardness measurements indicate respectively the thermal stability, optical transparency and mechanical stability of the grown crystals. Results of the non-linear optical measurements indicate the enhancement of second harmonic generation efficiency due to CdS addition. The DC and AC electrical measurements made in the temperature range 40-150^{0}C indicate an increase of the electrical parameters, viz. dielectric constant, dielectric loss factor and AC and DC electrical conductivities with the increase in temperature for all the six crystals studied.

Keywords: ADP crystal, Crystal growth, Doped crystals, Physical properties, X-ray diffraction.

I. INTRODUCTION

Ammonium dihydrogen phosphate ($NH_4H_2PO_4$) is a technologically important inorganic crystal and studies on ADP crystal attract interest because of their unique piezo-electric, antiferro-eletric, electro-optic, dielectric and nonlinear optical properties. Numerous applications of the nonlinear optical (NLO) property have been discussed in the field of science and technology in the past such as second, third and fourth harmonic generators for Nd: YAG, Nd: YLF lasers and for electro-optical applications such as Q-Switches for Ti: Sapphire, Alexandrite lasers, as well as for acousto-optical applications [1-7].

As a representative of hydrogen bonded material, ADP matrixes readily accept both organic and inorganic dopants. In the last decade numerous work has been done on the growth and characteristation of pure and doped (organic and inorganic) ADP crystals [8-13]. A series of organic dopants like ammonium malate [14], thiourea [15], L-lysine monohydrochloride dihydrate [16], L - alanine [17], L - arginine [18], ammonium acetate [19] and inorganic bimetallic impurities (Ni^{3+}, Mg^{2+}) [20] and their effects on various properties of ADP crystals were studied and authors reported that the addition of impurities in ADP crystal has turned various properties.

Recently intense research is being carried out in nanocrystals of semiconductors embedded in wide gap matrix like glass [21-23] and alkali halide matrices [24-26]. Also extensive work has been carried out on KDP doped with metal oxide impurity TiO_2 (nanoparticle) and has reported the gaint nonlinear optical response of TiO_2 (anatase) nanoparticles manifestation in KDP crystalline matrix [27-33].

Now a days the synthesis and the properties of highly luminescent II-VI compound semiconductor nanoparticles have been extensively investigated from the basic research point of view to the application field. With the miniaturization of the particles the band gap expands and the energy level of the core bands shift towards higher binding energy and subsequently, some physical properties change [34]. Electron and phonon confinement is possible by II-VI nanocrystalline semiconductors when the size of particles tend to be less than Bohr radius of the bulk crystal exciton showing new physical properties. These intriguing phenomena have been found to have new applications in telecommunication and transmission [35]. Bensouici et al [36,37] proved the possibility of embedding CdTe (a II-VI compound) nanoparticles in the crystalline matrix of KDP and alkali halide KBr. Also reports are available, on the doping of II-VI compound CdS (in nano form) embedded in alkali halides like KCl and NaCl [38,39].

Among various semiconductor nanoparticles nano-sized cadmium sulphide (CdS) particles have received much recognition as a potential candidate material for solar energy conversion [40,41], photo voltaic devices [42,43] and photo sensors [44] due to its large band gap (2.42 eV) at room temperature, good photo-conductivity, high absorption co-efficient which results in unusual electrical, optical, mechanical and magnetic properties due to the quantum confinement stimulated by size decreasing [45]. So it will be worthy and interesting to grow ADP single crystals with CdS as an impurity. Generally, ADP Single crystals are grown by the solution method at near ambient temperature. Normally II-VI compounds including CdS do not dissolve in water. Now the challenging yet interesting task is to identify a way to dissolve CdS and use it as a dopant in the growth of ADP single crystals. Very few reports are available which describe the preparation of water soluble CdS nanoparticles [46,47]. It has been reported that triglycine sulphate when doped with water-soluble CdS nanoparticle was found to have improved density and mechanical properties [48]. Tang et al [49] have reported the preparation of water soluble CdS by using ethylene diamine as a capping agent. Organic stabilizers are used to prevent the nanoparticles from aggregating by capping their surface during the wet chemical synthesis.

We have made efforts to introduce CdS as an impurity in the ADP crystal matrix. Ethylene diamine capped CdS nanoparticles were prepared by a solvothermal method using a domestic microwave oven (Mahadevan's method) [50-52]. Pure and CdS doped ADP single crystals (a total of six) were grown and characterized chemically, structurally, thermally, optically, mechanically and electrically by using the suitable standard methods. We herein report the results obtained and discussed.

II. EXPERIMENTAL PROCEDURE

2.1 Preparation of CdS nanoparticles

Analytical reagent (AR) grade cadmium acetate, thiourea, ethylene diamine, acetone and double distilled water were used in the study. Cadmium acetate and thiourea were dissolved in double distilled water in the presence of ethylene diamine to obtain ethylene diamine capped CdS nanoparticles following Mahadevan's method [50-52]. The solubility of the asprepared CdS nanoparticles is found to be 0.33g / 100ml H_2O.

2.2 Growth of ADP single crystals

Slow evaporation method was followed to grow pure and CdS doped ADP single crystals. 0.1g CdS nanoparticles were dissolved in 100ml double distilled water and used as the dopant. Five different dopant concentrations were considered by adding 1,2,3,4 and 5ml of the above solution to the ADP solution. The above doped solutions were stirred well and then allowed to equilibrate at room temperature in a dust free zone. In the beginning stage, small crystals appeared due to slow evaporation. They then grew larger in a considerable finite time. We represent the grown crystals in the same order as Pure ADP, CADP-1, CADP-2, CADP-3, CADP-4 and CADP-5.

2.3. Characterizations made

An automated X-ray powder diffractometer (X-PERT PRO PANnalytical) with monochromated CuK_α radiation (λ = 1.54056 Å) was used to collect the X-ray powder diffraction data in the 2θ range 10-70^0 for all the six powdered crystal samples. Procedures given by Lipson and Steeple [53] were followed to index all the reflection peaks. The lattice parameters were determined from the indexed data. The estimated standard deviations (e.s.d.s) were also determined. Fourier transform infrared (FTIR) spectra for the Pure ADP and ZADP-5 crystals were recorded by the KBr pellet method using a Perkin-Elmer FTIR spectrometer in the wavenumber range 400-4000cm^{-1}. Atomic absorption spectral (AAS) analysis was carried out for the doped crystals using an AAS spectrometer (Model AA-6300). Thermo gravimetric analysis (TGA) and differential thermal analysis (DTA) curves were obtained for the grown Pure and CADP-5 crystals using a thermal analyser (model SDT-Q600) in the nitrogen atmosphere in the temperature range of room temperature to 900^0C at a heating rate of 10^0C/min. UV-Vis-NIR transmission spectra for all the six crystals grown were recorded using a Perkin-Elmer Lambda 35 spectrophotometer in the wavelength range 190-1100nm. All the six crystals grown were subjected to second harmonic generation (SHG) test by the Kurtz and Perry [54] powder method using a Q-switched Nd:YAG laser (λ=1064nm) supplied by Spectra physics, USA. The mechanical property of all the six grown crystals were understood by carrying out the Vickers microhardness measurements on the (100) face using a SHIMADZU HMV-2T microhardness tester with a diamond indentor.

Crystals with large surface defect-free (i.e. without any pit or crack or scratch on the surface, tested with a traveling microscope) size (>3mm) were

selected and used for the measurements. AC and DC electrical measurements were carried out on all the six crystals along both a- and c- directions in the temperature range 40-150^{0}C. The extended portions of the crystals were removed completely and the opposite faces were polished and coated with good quality graphite to obtain a good conductive surface layer. The dimensions of the crystals were measured using a traveling microscope (Least count = 0.001cm). The observations were made while cooling the sample crystal and the temperature was controlled to an accuracy of $\pm 1^0$C.

The DC electrical conductivity measurements were carried out to an accuracy of $\pm$2% by the conventional two-probe method using a million megohm meter in a way similar to that followed by Mahadevan and his co-workers [55-57]. The DC conductivity (σ_{dc}) of the crystal was calculated using the relations:

$$\sigma_{dc} = d_{crys}/ (RA_{crys})$$

where R is the measured resistance, d_{crys} is the thickness of the sample crystal and A_{crys} is the area of the face of the crystal in contact with the electrode.

The capacitance (C_{crys}) and dielectric loss factor ($\tan\delta$) measurements were carried out to an accuracy of $\pm$2% by the parallel plate capacitor method using an LCR meter (Systronics make) with a fixed frequency of 1 kHz in a way similar to that followed by Mahadevan and his co-workers [58,59]. The air capacitance (C_{air}) was also measured but only at 40^{0}C since the temperature variation of C_{air} was found to be negligible. As the crystal surface area touching the electrode was smaller than the plate (electrode) area of the cell, the dielectric constant of the crystal (ε_r) was calculated using Mahadevan's formula [60,61].

$$\varepsilon_r = \left[\frac{A_{air}}{A_{crys}}\right]\left[\frac{C_{crys} - C_{air}[1 - A_{crys}/A_{air}]}{C_{air}}\right]$$

where C_{crys} is the capacitance with crystal (including air), C_{air} is the capacitance of air and A_{air} is the area of the electrode. The AC electrical conductivity (σ_{dc}) was calculated using the relation:

$$\sigma_{ac} = \varepsilon_0 \varepsilon_r \omega \tan\delta$$

where ε_0 is the permittivity of free space and ω is the angular frequency of the applied field.

III. Result and Discussion

3.1 Crystals grown

All the grown crystals were found to be stable, colour less and transparent. A photograph of the grown crystals is shown in Fig.1. The doped ADP crystals exhibit tetragonal morphology (the 12 faced scalenohedral) similar to that of the pure ADP crystal. Also, doping with CdS leads to improvement in the size of the crystals grown.

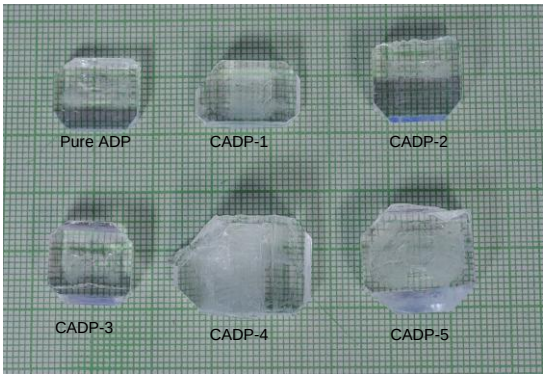

Fig:1-Photograph of Pure and CdS doped ADP single crystals

3.2 Lattice variation and chemical composition

The indexed PXRD patterns observed in the present study are shown in Figure 2. Appearance of strong and sharp peaks confirms the crystalline nature of the grown crystals. The average lattice parameters obtained from PXRD data are provided in Table 1.

Table:1- The observed lattice parameters and AAS data for all grown crystals

Crystal	Lattice parameters			Cd atom content (ppm)
	a (Å)	c (Å)	Volume (Å^3)	
Pure ADP	7.490 (1)	7.549 (6)	423.5	--
CADP-1	7.502 (2)	7.554 (9)	425.1	0.30
CADP -2	7.532 (1)	7.532 (10)	427.3	0.50
CADP -3	7.556 (1)	7.544 (1)	430.7	3.02
CADP -4	7.573 (7)	7.655 (5)	439.0	2.72
CADP -5	7.569 (1)	7.685 (8)	442.3	3.62

The average lattice parameters observed in the present study (see Table 1) for the pure ADP crystal agree well with that reported in the literature [62]; a=7.502Å and c =7.554 Å. This confirms the identity of the substance. The observed increase of lattice volume caused by the impurity addition indicates that the impurity molecules have entered into the ADP crystal matrix. Moreover, it can be seen that the lattice volume varies further with the increase in impurity concentration which indicates the inclusion of the dopant. Atomic Absorption Spectral (AAS) study confirms and provides the amount of dopant (Cd metal ion) present in the doped ADP crystals. The Cd atom contents observed from the AAS study are given in Table 1. So, the present study indicates that it is possible that CdS can be doped to ADP crystal.

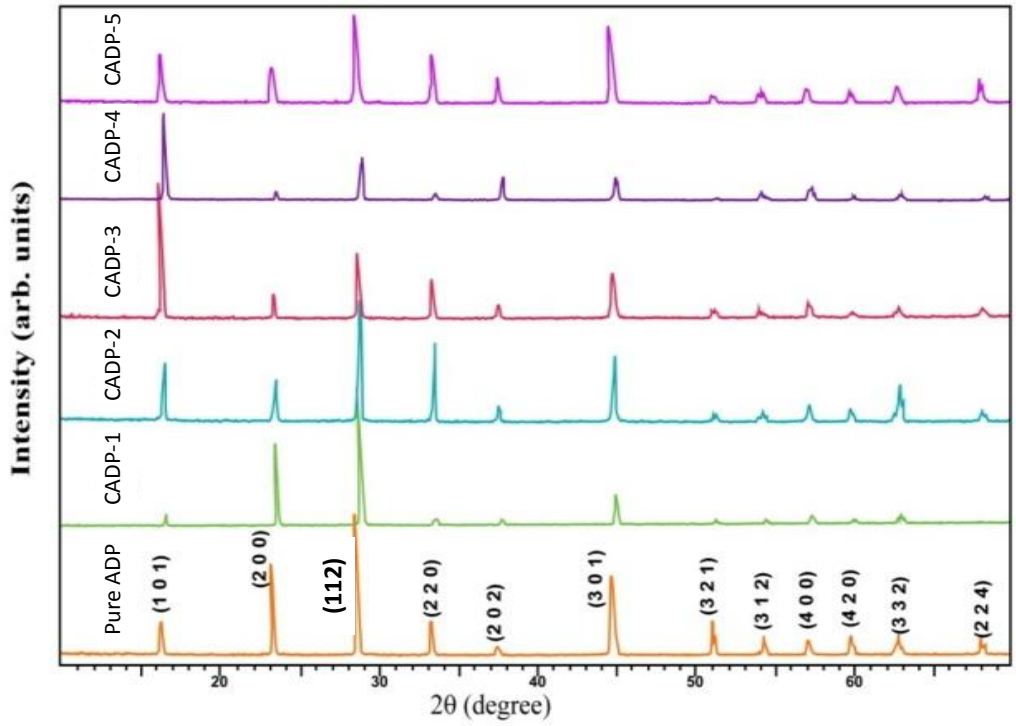

Fig-2: PXRD patterns observed for the pure and CdS doped ADP crystals

Figure 3 shows the FTIR spectra observed for the Pure ADP and CADP-5. The vibrational band assignments are provided in Table 2. Significant difference could not be observed for the doped crystals as the impurity concentrations considered are small. The spectrum observed for the pure ADP compares well with that reported in the literature which again confirms the material of the crystal. The vibrational band assignments reported for pure ADP in the literature [63] are also given in Table 2 for comparison.

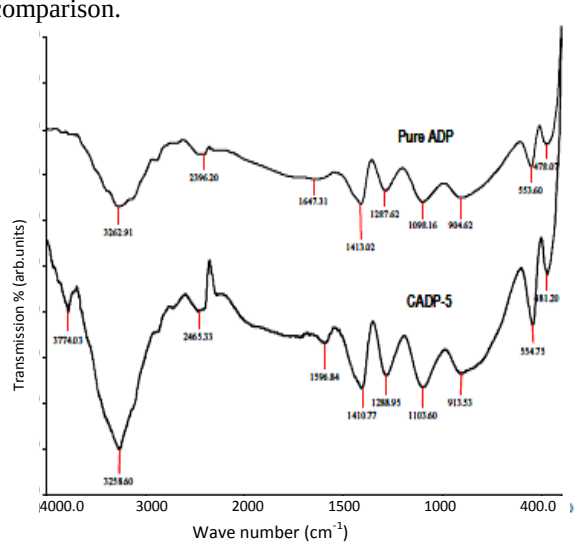

Fig:3-FTIR spectra observed for the Pure ADP and CADP-5 crystals

Table:2-Vibrational band assignments

Wave number (cm^{-1}) for			Assignment
Pure ADP [Present]	CADP -5	Pure ADP [63]	
3262	3258	3140	O-H Stretching
2396	2465	2370	Combination band of stretching
1647	1596	1646	N-H bonding of NH_4
1413	1410	1402	Bending stretching of NH_4
1287	1288	1293	Combination band of stretching
1098	1103	1100	P-O-H stretching
904	913	930	P-O-H stretching
553	554	544	PO_4 stretching
478	481	470	PO_4 stretching

3.3 Thermal stability

The TGA and DTA curves obtained for pure ADP and CADP-5 are shown in Figure 4 [(a) and (b)]. It can be understood that pure ADP and CADP-5 are thermally stable at least up to 201.8^0C and 200.2^0C respectively. The decomposition takes place at (about) these temperatures. The difference in thermal stability observed between these two crystals makes us to understand that CdS molecules have entered into the ADP crystal matrix in the case of doped crystals.

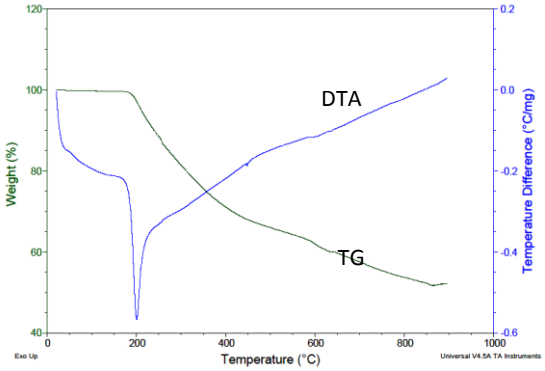

Fig:4(a)-TG/DTA Curve for Pure ADP

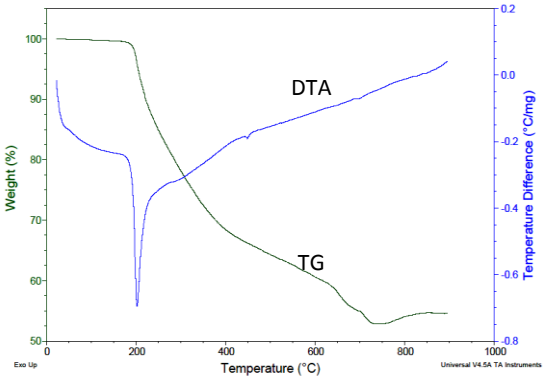

Fig:4 (b)-TG/DTA Curve for CADP-5

3.4 Optical and mechanical properties

The UV-Vis-NIR spectra observed in the present study for all the six crystals grown are shown in Figure 5. The observed optical transmission percentages and cut off wavelengths are given in Table 3. The UV-Vis-NIR spectra indicate that both pure and CdS doped ADP crystals exhibit good transmittances towards the visible and infrared regions and low cut off wavelengths. The observed transparent nature of these crystals is a desirable property for the grown crystals to have NLO applications.

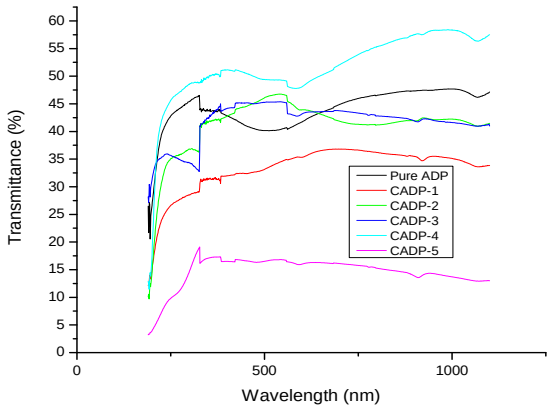

Fig-5: UV-Vis-NIR spectra observed for the Pure and CdS doped ADP crystals

The second harmonic generation (SHG) efficiencies observed are provided in Table 3. It is found that the SHG efficiency increases significantly due to CdS doping. In effect, the results obtained indicate that all the six crystals grown in the present study are NLO active.

Table-3: The cut off wave lengths, optical transmission percentages, SHG efficiencies and work hardening coefficients (n)

Crystals	Cutoff wave length (nm)	Optical transmission (%)	SHG efficiency (in ADP unit)	Work hardening co-efficient
Pure ADP	331	46	1.00	3.32
CADP-1	328	37	4.10	2.90
CADP -2	320	41	4.00	3.33
CADP -3	313	43	4.28	2.87
CADP -4	305	57	4.32	1.35
CADP -5	300	16	3.88	3.33

The hardness of a material is a measure of its resistance it offers to local deformation and micro-indentation test is a useful method for understanding the nature of plastic flow and its influence on the deformation of the materials [64].

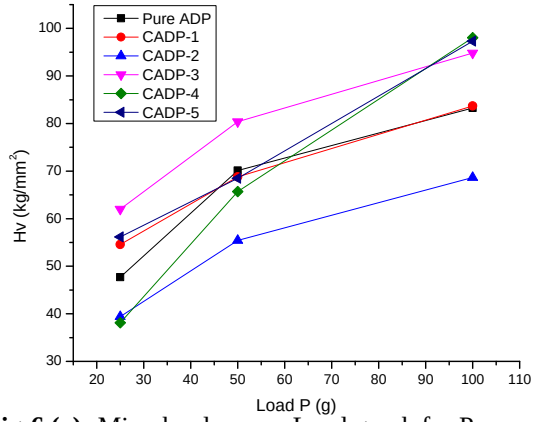

Fig-6 (a): Microhardness vs Load graph for Pure and CdS doped crystals

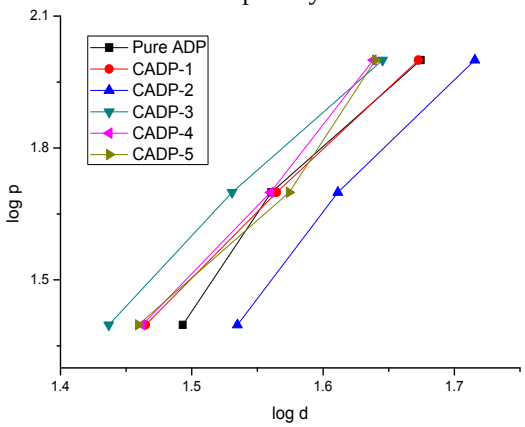

Fig-6 (b): Log P vs log d plots for the pure and CdS doped crystals

The micro-identation test is a useful method for studying the nature of plastic flow and its influence on the deformation of the materials. Higher hardness value of a crystal indicates that greater stress is required to create dislocation [65]. Figure 6 (a) shows the variation of Vicker hardness number (H_v) with applied load (P) for the pure and CdS doped ADP crystals grown in the present study.

The log P versus log d plots (d is the average diagonal length of the indentation made) were also made and are shown in Figure 6 (b). The plots are found to be nearly straight line. From the slope of the best fitted lines, the work hardening coefficients or Mayer indices (n) were obtained and are given in Table 3.

Results obtained in the present study indicates that the H_v value increases with the increasing load for all the six crystals grown. The H_v value increases up to a load of 100g, above which cracks start developing which may be due to the release of internal stress generation with indentation. The Vicker hardness number (H_v) is defined as

$$H_v = 1.8544\ P/d^2\ kg/mm^2$$

and the Mayer's law [66] is expressed as

$$P = k_1 d^n$$

where k_1 is the material constant.

According to Onitsch and Hanneman 'n' should lie between 1.0 and 1.6 for hard materials and above 1.6 for soft ones [66]. The 'n' values observed in the present study are more than 1.6. This indicates that all the six crystals grown belong to soft materials category.

3.5 Electrical properties

The dielectric parameters, viz. DC electrical conductivity (σ_{dc}), dielectric constant (ε_r), dielectric loss factor $(\tan\delta)$ and AC conductivity (σ_{ac}) values obtained in the present study are shown in Figures 7-10. It can be seen that all the four parameters increase with the increase in temperature. However, no systematic variation is observed with the impurity concentration (volume of CdS solution added to the ADP solution used for the growth of single crystals) for all the above electrical parameters in the whole temperature range considered in the present study. This is illustrated in Figures 11-14. The DC conductivity is more or less same along a- and c-directions. Other electrical parameters viz. ε_r , $\tan\delta$ and σ_{ac} increase with the increase in temperature and the values of doped crystals are mostly more than that of the pure ADP for both the directions (a- and c-). But the variation with impurity concentration is non-linear.

Plots between ln σ_{dc} and 10^3/T and between ln σ_{ac} and 10^3/T (not shown here) are found to be nearly linear. So, the conductivity (DC and AC) values were fitted correspondingly to the Arrhenius relation.

$$\sigma_{dc} = \sigma_{0dc}\exp[-E_{dc}/(kT)]$$
$$\sigma_{ac} = \sigma_{0ac}\exp[-E_{ac}/(kT)]$$

where σ_{0dc} and σ_{0ac} are the proportionality constants (considered to be the characteristic constants of the material), k is the Boltzmann constant and T is the absolute temperature. The DC and AC activation energies (E_{dc} and E_{ac}) were estimated using the slopes of the corresponding line plots. The estimated DC and AC activation energies for the pure and CdS doped ADP crystals grown in the present study are given in Table 4. The E_{dc} values are observed to be more than the E_{ac} values as expected. The low values of E_{dc} and E_{ac} observed suggests that oxygen vacancies may be responsible for conduction in the temperature region considered in the present study.

Table-4: The activation energies (E_{dc} and E_{ac}) estimated for the pure and CdS doped ADP crystals

Crystal	Activation energies (eV)			
	Along a - direction		Along c - direction	
	E_{ac}	E_{dc}	E_{ac}	E_{dc}
Pure ADP	0.111	0.275	0.163	0.270
CADP-1	0.119	0.234	0.178	0.405
CADP -2	0.065	0.265	0.118	0.297
CADP -3	0.057	0.281	0.125	0.271
CADP -4	0.069	0.279	0.120	0.293
CADP -5	0.069	0.235	0.105	0.215

Variation of dielectric constant with temperature is generally attributed to the crystal expansion, the electronic and ionic polarizations and the presence of impurities and crystal defects. The variation of ε_r at low temperature is mainly due to the crystal expansion and electronic and ionic polarisations. The increase of ε_r at higher temperatures is mainly attributed to the thermally generated charge carriers and impurity dipoles. It has been shown by varotsos [67] that the electronic polarizability practically remains constant in the case of ionic crystals. So, the increase in dielectric constant with temperature observed in the present study is essentially due to the temperature variation of ionic polarizability.

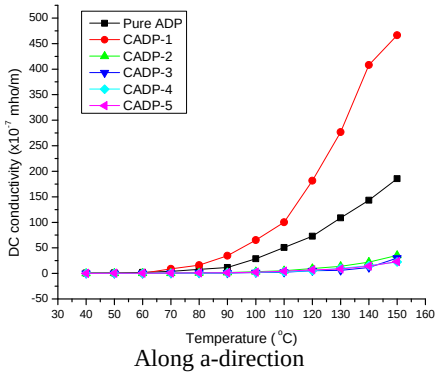

Along a-direction

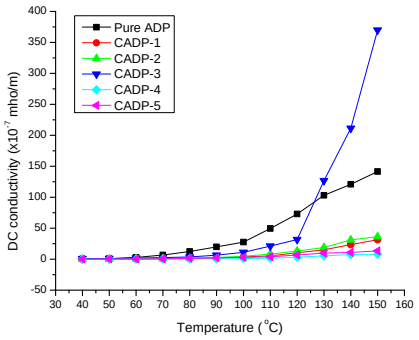

Along c-direction

Fig.7: DC electrical conductivities (σ_{dc}) observed for the pure and CdS doped ADP crystals

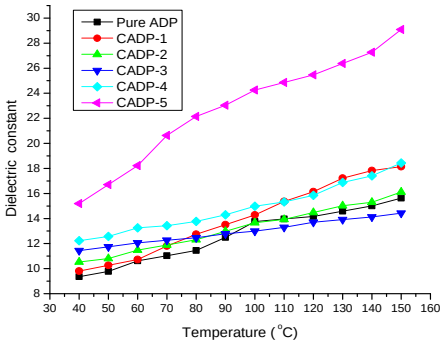

Along a-direction

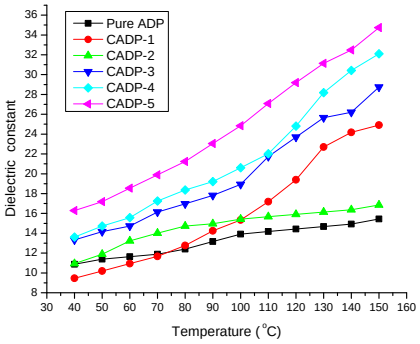

Along c-direction

Fig.8: Dielectric constants (ε_r) observed for the pure and CdS doped ADP crystals

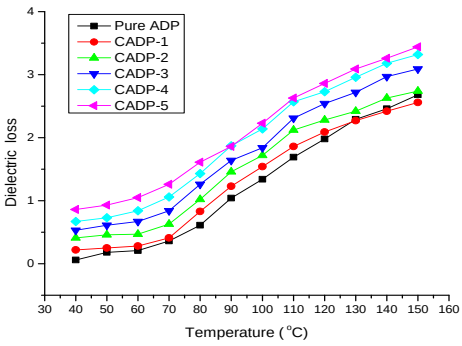

Along a-direction

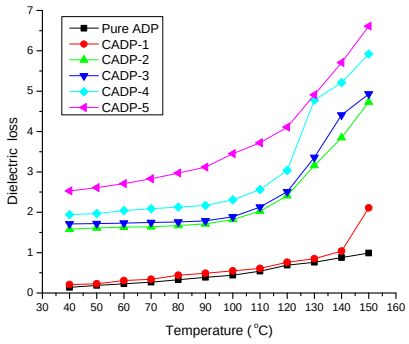

Along c-direction

Fig.9: Dielectric loss factors (tan δ) observed for the pure and CdS doped ADP crystals

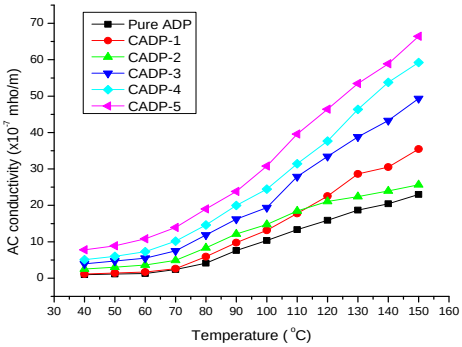

Along a-direction

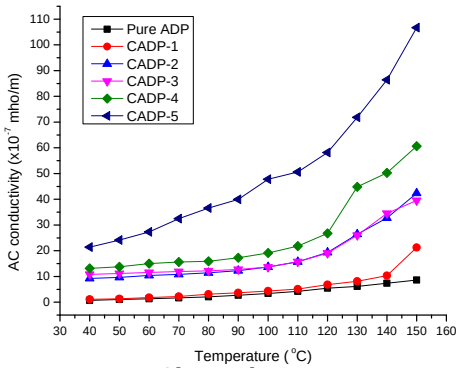

Along c-direction

Fig.10: AC electrical conductivities (σ_{ac}) observed for the pure and CdS doped ADP crystals

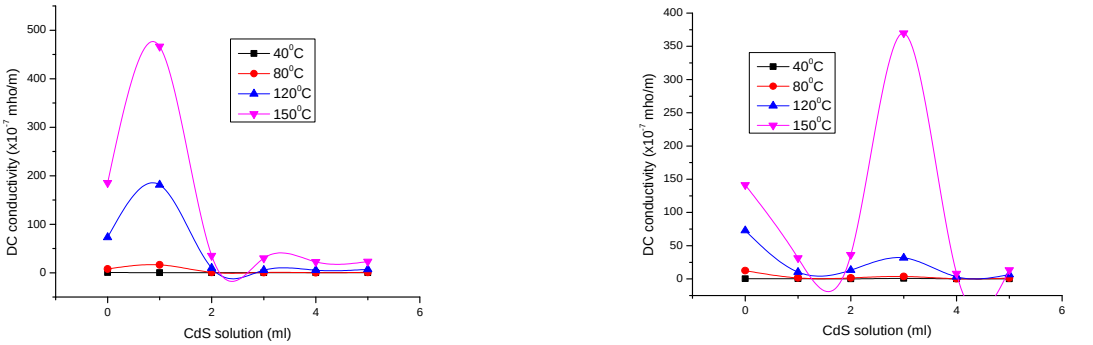

Along a-direction Along c-direction

Fig.11: Impurity concentration dependence of σ_{dc} observed for the pure and CdS doped ADP crystals

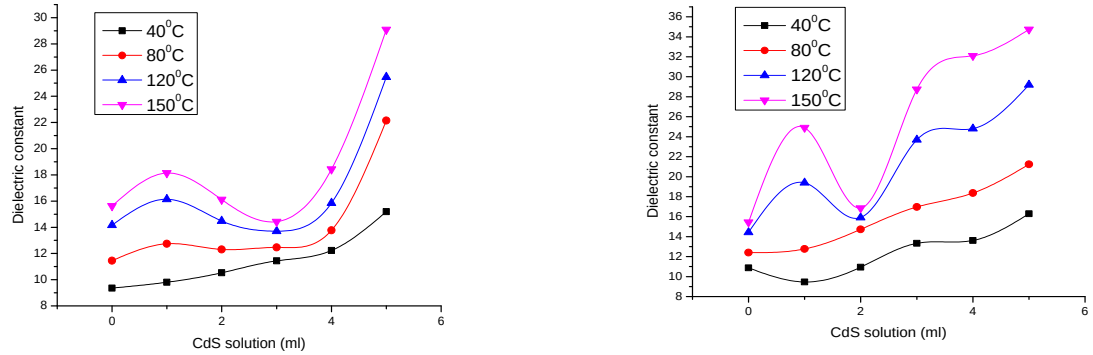

Along a-direction Along c-direction

Fig.12: Impurity concentration dependence of ε_r observed for the pure and CdS doped ADP crystals

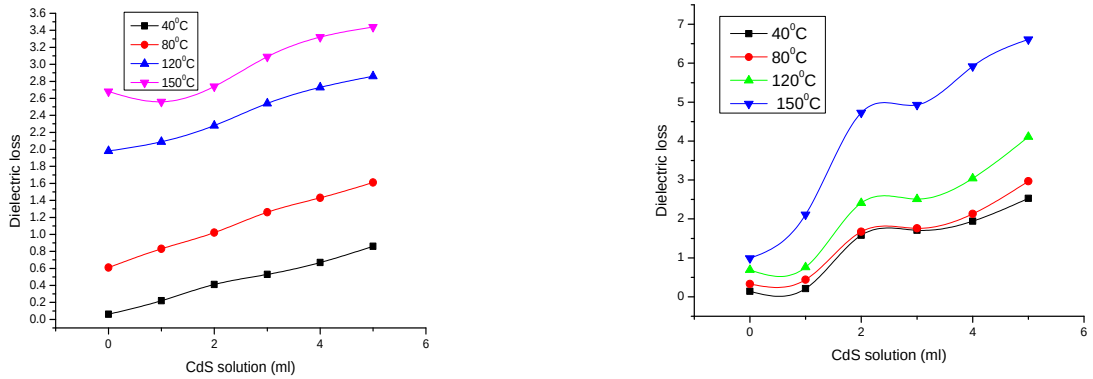

Along a-direction Along c-direction

Fig.13: Impurity concentration dependence of tan δ observed for the pure and CdS doped ADP crystals

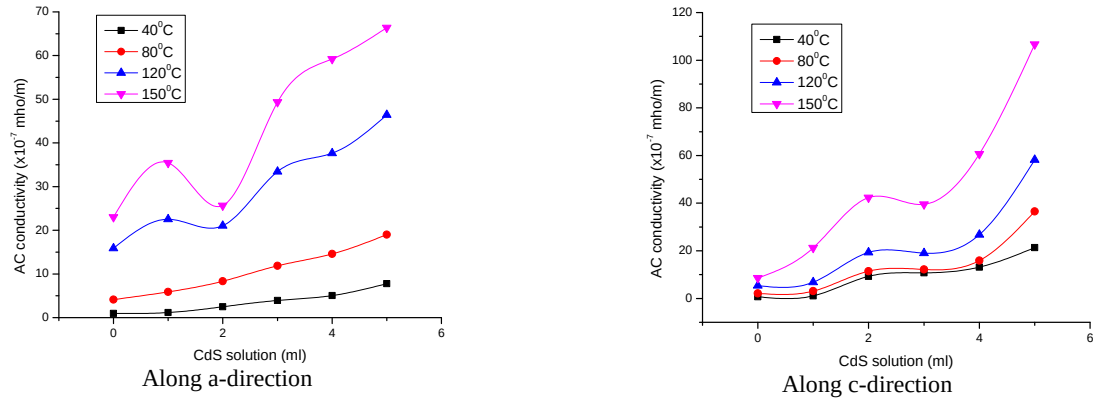

Along a-direction Along c-direction

Fig.14: Impurity concentration dependence of σ_{ac} observed for the pure and CdS doped ADP crystals

The CdS is an ionic substance and is expected to became Cd^{2+} and S^{2-} ions in the solution. In the ADP crystal matrix, some of these ions are expected to occupy interstitial positions. This induces bulk defect states due to competition in getting the sites for the impurity ions to occupy. To some extent, the impurity ions are expected to replace the ions in ADP. So, it is expected to create a random disturbance in the hydrogen bonding system in the ADP crystal matrix. As the conduction in ADP crystal is protonic, the random disturbance in the hydrogen bonding system may cause the electrical parameters to vary nonlinealy with the impurity concentration.

IV. CONCLUSION

CdS nanoparticles were synthesized by a simple solvothermal method and using ethylene diamine as a capping agent and thus prepared CdS was found to be slightly soluble in water. Its solubility was found to be 0.33g/ 100ml of water. Good quality single crystals of CdS doped ammonium dihydrogen phosphate (ADP) have been grown by the slow evaporation technique at room temperature. All the grown crystals were characterized. Results obtained shows that the impurity molecules have entered into the ADP crystal matrix. There is significant enhancement of SHG efficiency. Moreover, CdS doping helped in tuning the optical and electrical properties of ADP crystal.

REFERENCES

[1]. S.R.Marder, B.G.Tiemann, J.W.Perry, et.al., *Materials for Non-linear optical chemical perspectives* (American Chemical Society, Washington, 1991).
[2]. H.M.Muncheryan, *Lasers and opto-Electronics Devices* (Hemisphere Pub. Co, New York, 1991).
[3]. Y.R.Shen, *The Principles of Non linear optics* (Wiley, New York, 1984).
[4]. P.Meystrey and M.Sargent, *Elements of Quantum optics* (Springe – Verlag, Berlin, 1991).
[5]. J.I.Sakai, *Phase conjucate optics* (Mc Graw Hill, Inc., New York, 1992).
[6]. P.Ramasamy and P.Santhana Raghavan, *Crystal Growth Process and Methods* (KRV Publications, Kumbakonam, 1999).
[7]. P.Santhana Raghavan and P.Ramaswamy, *Recent Trends in Cryst. Growth* (Pinsa 68, New Delhi, 2002).
[8]. A.Anne Assencia and C.Mahadevan, *Bull of Mater. Sci., 28,* 2005, 415.
[9]. D.L.Xu and D.F.Xue, *J. of Cryst. Growth, 286,* 2006, 108.
[10]. N.P.Rajesh, V.Kannan, P.Santhana Raghavan, P.Ramaswamy and C.W.Lan, *Mater. Chem. and Phy., 76,* 2002, 181.
[11]. J.W.Mullin, A.Amatavivadhana, *App. Chem., 17,* 1967, 151.
[12]. P.Rajesh and P.Ramaswamy, *Mater. Lett., 63,* 2009, 2260.
[13]. P.V.Dhanaraj, G.Bhagavanarayana and N.P.Rajesh, *Mat. Chem. Phys., 112,* 2008, 490.
[14]. P.Rajesh, P.Ramasamy, G.Bhagavannarayana, *J.Cryst Growth, 311,* 2009, 4069.
[15]. A.Jayarama, S.M.Dharmaprakash, *Indian J.Pure and App. Phys., 43,* 2005, 859.
[16]. P.Rajesh, P.Ramaswamy, C.K.Mahadevan *J.Cryst. Growth, 311,* 2009, 1156.
[17]. Ferdousi Akhtar and Jiban Podder, *J. of Cryst. Process and Tech., 1,* 2011, 18.
[18]. G.G.Muley, M.N.Rode, S.A.Waghuley, B.H.Pawar, *optoelectronics and advan. Mater., 4,* 2010, 11-14.
[19]. P.Rajesh, K.Boopathi, P.Ramasamy, *J. Cryst. Growth, 318,* 2011, 751.
[20]. A.Claudc, V.Vaithianathan, R.Bairava Ganesh, R.Sathya Lakshmi, P.Rama samy, *J. App. Sci., 6 (1),* 2006, 85.
[21]. T.M.Hayes, L.B.Lurio, J.Pant, P.D.Persans, *Solid State Commun., 117,* 2001, 627.
[22]. P.Maly, T.Miyoshi, *J.Lumin., 90,* 2000, 129.
[23]. A.Medrum, C.W.White, L.A.Boatner, I.M.Anderson, R.A.Zuhr, E.Sonder, J.D.Budai, D.O.Anderson, *Nucl. Ins. Meth. Phys. Res., B 148,* 1999, 957.
[24]. J.Zhao, M.Ikezawa, A.V.Ferderov, Y.Masumoto, *J.Lumin., 525,* 2000, 87.
[25]. M.Haselhoff, K.Reimann, H.J.Weber, *J.Cryst. Growth, 196,* 1999, 135.
[26]. H.Harada, H.Kondo, N.Ichimura, S.Hashimoto, *Jpn. J.Appl. Phys., 38,* 1999, 1318.
[27]. V.Ya.Gayvoronsky, V.N.Starkov, M.A.Kopylovsky, M.S.Brodyn, E.A.Vishnyakov, A.Yu.Boyarchuk, I.M.Pritula, *Ukr. J.Phys., 55,* 2010, 875.
[28]. V.Ya.Gayvoronsky, M.A.Kopylovsky, V.O.Yatsyna, A.S.Popov, A.v.Kosinova, I.M.Pritula, *Functional Mater., 19,* 2012, 54.
[29]. Valentin G.Grachev, Ian.A.Vrable, Galina, I.Malovichko, Igor M.Pritula, Olga N.Bezkrovnaya, Anna V.Kosinova, Vasyl O.Yatsyna and Vladimir, Ya.Gayvoronsky, *J. Appl. Phys. 112,* 2012, 014107 (1-10).

[30]. I.Pritula, V.Gagvoronskg, M.Kopylovskg, M.Kolybaeva, V.Puzikov, A.Kosinova, V.T.Kachenko, V.Tsurikov, T.Konstantiniva, V.Pogibko, *Functional Mater., 15,* 2008, 420.
[31]. V.Ya.Gayvoronsky, M.A.Kopylovsky, M.S.Brodyn, I.M.Pritula, M.I.Kolybaeva and V.M.Puzikov, *Laser Phys. Lett., 10,* 2013, 1.
[32]. I.Pritula, O.Bezkrovnaya, M.Kolybayeva, A.Kosinova, D.Sofronov, V.Tkachenko, V.Tsurikov, *Mater. Chem. Phys., 129,* 2011, 777.
[33]. V.Ya.Gayvoronsky, M.A.Kopylovsky, V.O.Yatsyna, A.I.Rostotsky, M.S.Brodyn, I.M.Pritula, *Ukr .J. Phys., 57,* 2012, 159.
[34]. Chang Q.Sun, B.K.Tay, S.Li, X.W.Sun, S.P.Lau, T.P.Chen, *Mater. Phys. Mech., 129,* 2001, 4.
[35]. O.Conde, A.G.Rolo, M.J.M.Gomes, Ricolleau, D.J.Barber, *J. Cryst. Growth, 371,* 2003, 247.
[36]. A.Bensouici, J.L.Plaza, O.Halimi, B.Boudine, M.Sebais, E.Dieguez, *J. optoelectronics and Adv. Mater., 10,* 2008, 3051.
[37]. A.Bensouici, J.L.Plaza, E.Dieguez, O.Halimi, B.Boudine, S.Addala, L.Guerbous, M.Sebais, *J. Lumin., 129,* 2009, 948.
[38]. B.Boudine, M.Sebais, O.Halimi, R.Mouras, A.Boudrioua, P.Bourson, *Optical Mate., 25,* 2004, 373.
[39]. B.Boudine, M.Sebais, O.Halimie, H.Alliouche, A.Boudrioua, R.Mouras, *Catalysis Today, 89,* 2004, 293.
[40]. G.Sasikala, P.Thilakan and C.Subramaniam, *Sol. Energy Mater. Sol. Cells***.,** *62,* 2000, 275.
[41]. C.Thanachayanout, K.Inpor, S.Sahasithiwat and V.Meeyoo, *J.Korean Phys. Soc.,* 52, 2008, 1540.
[42]. C.S.Ferekides, D.Marinskly, V.Viswanathan, B.Tetaly, V.Palekis, P.Selvaraj and D.L.Morel, *Thin Solid Films, 361,* 2000, 520.
[43]. J.Britt and C.Ferekides, *Appl. Phys. Lett.,* 62, 1993, 22.
[44]. B.K.Maremadi, K.Colbow and Y.Harima, *Rev. Sci. Instrum,* 68, 1997, 3893.
[45]. A.G.Rolo, L.G.Vieira, M.J.M.Gomes, J.L.Ribeiro, M.S.Belsley, M.P.Dos Santos. *Thin solid films,* 1998, 312-348.
[46]. Y.Andrew wang, J.Jack Li, Haiyan Chen, Xiaogang Peng, *J. Am. Chem. Soc., 124,* 2002, 2293.
[47]. Wenzhou Guo, J.Jack Li, Y.Andrew Wang, Xiaogang Peng, *Chem. Mater., 15,* 2003, 3125.
[48]. K.Balasubhramanian, P.Selvarajan and E.Kumar, *Indian J. Sci. and Technology, 3 (1),* 2010, 41.
[49]. Tang, Mi Yan, Hui zhang, Minzhe xia, Daren Yang, *Mater. Lett., 59,* 2009, 1024.
[50]. R.S.S.Saravanan and C.K.Mahadevan J.Alloys and Compounds, *541,* 2012, 115.
[51]. S.I.Srikrishna Ramya and C.K.Mahadevan, *Mater. Lett., 89,* 2012, 111.
[52]. S.Nagaveena and C.K.Mahadevan, *J.Alloys and Compounds, 582,* 2013, 447.
[53]. H.Lipson, H.Steeple, *Interpretation of X-ray powder diffraction patterns,* (Mac Milan, Newyork, 1970).
[54]. S.K.Kurtz, T.T.Perry, *J. Appl. Phys., 39,* 1968, 3798.
[55]. T.H.Freeda, C.K.Mahadevan, *Bull. Mater. Sci., 23,* 2000, 335.
[56]. S.Perumal and C.K.Mahadevan, *Physics B, 367,* 2005, 172.
[57]. G.Selvarajan, C.K.Mahadevan, *J. Mater. Sci., 41,* 2006, 8218.
[58]. S.Goma, C.M. Padma and C.K. Mahadevan, *Mater. Lett., 60,* 2006, 3701.
[59]. N.Manonmani, C.K. Mahadevan and V.Umayourbhagan, *Mater. Manuf. Process, 22,* 2007, 388.
[60]. M.Meena, C.K.Mahadevan, *Cryst. Res. Technol., 43,* 2008, 116.
[61]. M.Priya, C.K.Mahadevan, *Physica B, 403,* 2008, 67.
[62]. S.Chaki, M.P.Deshpande, J.P.Tailor, M.D.Chaudhary, K.Mahato, *Am. J. condensed Matter Phys., 2 (1),* 2012, 22.
[63]. P.V.Dhanaraj, N.P.Rajesh, *Crystallisation and material Science of Modern artificial and natural crystals* (Edited by Dr.Elena Borisenko, Pp.79, 2012)
[64]. M.V.Artemyev, V.Sperling, U.Woggon, *J. Appl. Phys., 81 (10),* 1997, 6975.
[65]. P.Rajesh, P.Ramaswamy, *Physica B, 404,* 2009, 1611.
[66]. S.Karan, S.P.Sen Gupta, *Mater. Sci. Eng., A398,* 2005, 198.